Far Infrared Spectra and Internal-Rotation Potential of Ethyl Methyl Ether

Teizo KITAGAWA, Keiichi OHNO,* Hiromu SUGETA, and Tatsuo MIYAZAWA

Institute for Protein Research, Osaka University, Yamada-kami, Suita, Osaka

(Received April 14, 1971)

Far infrared spectra (700~40 cm^{-1}) of ethyl methyl ether and deuterated species ($CH_3CH_2OCD_3$, $CD_3CH_2OCH_3$, $CH_3CD_2OCH_3$, and $CD_3CD_2OCH_3$) were measured in the crystalline, liquid and gaseous states and carbon tetrachloride solution. A low temperature cell was constructed for measuring far infrared absorption of highly volatile samples in the liquid and crystalline states. Far infrared bands due to skeletal bending vibrations of the trans and gauche isomers and lattice vibrations were assigned. From analyses of isotope effects on infrared frequencies, internal-rotation vibrations of the CH_3-CH_2, CH_2-O, and O-CH_3 bonds of the trans isomer of ethyl methyl ether were found at 248, 115, and 202 cm^{-1}, respectively, in the gaseous state. Normal vibrations were treated with the local-symmetry force field and force constants were adjusted by the method of least squares. By the use of Mathieu equation, the threefold potential barriers of the methyl groups of the trans isomer were estimated as $V_3(CH_3\text{-}C)=3.3\pm0.1$ and $V_3(O\text{-}CH_3)=2.5\pm0.1$ kcal/mol.

Studies of the internal-rotation about the CH_2-O bond of the C-CH_2-O-C group are important for treating chain conformations of polyethers including polyethylene glycol[1] $[\text{-}CH_2\text{-}CH_2\text{-}O\text{-}]_p$. The molecule of ethyl methyl ether CH_3-CH_2-O-CH_3 serves as an appropriate model for studying the internal rotation about CH_2-O bonds.

Analyses of the infrared and Raman spectra[2-5] of ethyl methyl ether suggested that the trans and gauche isomers coexist in the gaseous state and liquid state while the trans isomer remains in the crystalline state. The coexistence of rotational isomers was confirmed by the measurement of the temperature effect on the infrared spectra[6]. Furthermore, from the relative intensity of the infrared bands at ~375 cm^{-1} and ~280 cm^{-1}, the energy difference between the gauche and trans isomers was estimated as 1.5 kcal/mol in the gaseous and liquid states[6]. The electron diffraction of gaseous molecules of ethyl methyl ether was analysed[7] and the predominant isomer was confirmed to be trans and also the weak peaks due to the gauche isomer were recognized in the radial distribution. The molecular structure of the trans isomer was determined precisely by the analyses of the microwave spectra[8]. Recently, the infrared and Raman spectra (3000~500 cm^{-1}) of eight isotopic species of ethyl methyl ether were measured and, from the relative intensity of the infrared bands at 1015 cm^{-1} and 980 cm^{-1}, the energy difference between the gauche and trans isomers was estimated as 1.35 kcal/mol[9].

Vibrational frequencies of internal-rotation modes are important for studying internal-rotation potential. Accordingly, for establishing vibrational assignments of the internal-rotation frequencies of ethyl methyl ether $[CH_3CH_2OCH_3(d_0)]$ and deuterated species $[CH_3CD_2OCH_3(d_2)$, $CD_3CH_2OCH_3(d_3)$, $CH_3CH_2OCD_3$ (d_3') and $CD_3CD_2OCH_3(d_5)]$, the far infrared spectra of the gaseous, liquid and crystalline states were measured in the present study. A low-temperature cell was constructed for measuring far infrared spectra of liquid and crystalline phases of highly volatile samples since the boiling point (6°C) of ethyl methyl ether was lower than room temperature.

Experimental

Ethyl methyl ether and deuterated species were synthesized with Williamson's method. Starting material of ethyl alcohol was prepared, in advance, by the reduction of acetyl chloride with lithium aluminum hydride (or deuteride)[10]. Samples of ethyl methyl ether and deuterated species were purified by repeated distillation from dry ice temperature to liquid nitrogen temperature in vacuum. The samples were dried over phosphorous pentoxide just before spectroscopic measurements and were transferred into absorption cells through vacuum line.

Infrared spectra in the 700~200 cm^{-1} region were recorded on a Hitachi EPI-L Infrared Spectrophotometer. Cesium iodide crystal plates of 3 mm thickness were used as windows of absorption cells. For the 400~50 cm^{-1} region, a Hitachi FIS-3 Far Infrared Spectrophotometer was used with absorption cells of polyethylene windows.

Low Temperature Cell. Figure 1 shows the low-temperature cell constructed in the present study for far infrared measrements. The cryostat consists of Parts A and B. Part A is the outer jacket and is held, with a fringe (1), on the cover of the sample compartment of the spectrophotometer. The fringe is fastened onto the cover (2) with an O-ring and screws, and polyethylene sheets of 1 mm thickness are used as optical windows (3). Part B is the inner jacket and is fastened to Part A with an O-ring and screws. The liquid nitrogen reservoir (4) is as large as 1.8 *l*. The copper block (5) is provided with a channel so that liquid nitrogen is led to the bottom part of the block. However, a small temperature difference is found between the copper block (5) and the sample (6) so that a copper constantan thermo-

* Present address: Department of Chemistry, Faculty of Science, Hiroshima University, Higashi-sendamachi, Hiroshima.

1) T. Miyazawa, K. Fukushima, and Y. Ideguchi, *J. Chem. Phys.*, **37**, 2764 (1962); H. Tadokoro, Y. Chatani, T. Yoshihara. S. Tahara, and S. Murahashi, *Makromol. Chem.*, **73**, 109 (1964); H. Matsuura and T. Miyazawa, *J. Polymer Sci., A-2*, **7**, 1735 (1969).

2) K. W. F. Kohlrausch, *Monatsh. Chem.*, **68**, 349 (1936).

3) Y. Mashiko, *Nippon Kagaku Zasshi*, **80**, 593 (1959).

4) R. G. Snyder and G. Zerbi, *Spectrochim. Acta*, **23A**, 391 (1967).

5) A. D. H. Clague and A. Danti, *ibid.*, **24A**, 439 (1968).

6) T. Kitagawa and T. Miyazawa, This Bulletin, **41**, 1976 (1968).

7) M. Abe, PhD dissertation, the University of Tokyo (1968).

8) M. Hayashi, H. Imaishi, K. Ohno, and H. Murata, This Bulletin, **44**, 299 (1971).

9) J. P. Perchard, *Spectrochim. Acta*, **26A**, 707 (1970).

10) J. D. Cox and H. S. Turner, *J. Chem. Soc.*, **1950**, 3176.

couple is embedded into the window (polyethylene or silicon) of the sample cell. Thermocouple wires are connected outside through hermetic seals (7). The cryostat is evacuated better than 10^{-5} mmHg.

Double-Chopping Operation. In the far infrared region, the emission from the optical wedge in the reference beam of a double-beam spectrophotometer is not negligible as compared with the emission from the far infrared source. When the temperature of the sample in the sample beam is kept low, the emission difference between the wedge and the sample is also compensated by the wedge itself and the transmittance recorded on the chart is appreciably lower than the true transmittance. Accordingly, in the present study, the double-chopping mode (0.9 cps) of FIS-3 was used for absorption measurements of the liquid and crystalline phases at low temperatures and the systematic error due to the wedge emission was eliminated.

Solid Spectra. For absorption measurements of deposited solid, a silicon disk [(6) in Fig. 1] is held on the copper block (5). A glass jet opening is connected to a metal tube (8) so that the sample gas may be introduced from outside onto the silicon disk. Sample gas of ethyl methyl ether was deposited on the silicon disk at 77°K and was then annealed at temperatures as high as 150°K. Far infrared spectra of the solid phase at 77°K are shown in Fig. 2, where transmittance curves of deposited unannealed sample are shown with broken lines and curves of annealed sample are shown with solid lines.

Liquid Spectra. For absorption measurements of condensed liquid, a vacuum tight polyethylene cell (0.2 mm thick) was constructed by welding polyethylene sheets and tubes (entrance and exit). The cell is held on the copper block (5) of the cryostat (Fig. 1) and the entrance and exit are connected to the metal tubes (8). The sample of ethyl methyl ether is introduced through a metal tube and entrance polyethylene tube, and is liquified inside the polyethylene cell kept at low temperature.

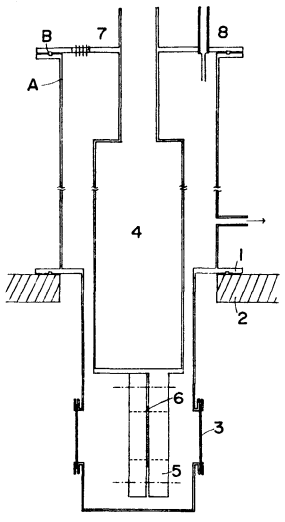

Fig. 1. Cryostat for far infrared absorption measurements.

Far infrared spectra of the liquid phase at ~170°K are shown in Fig. 3. The weak band at 78 cm^{-1} is due to polyethylene sheets of the liquid cell. Since low frequency modes are appreciably influenced by intermolecular interactions, observed peak frequencies of liquid spectra (Fig. 3) are appreciably lower than corresponding peak frequencies of the solid spectra (Fig. 2).

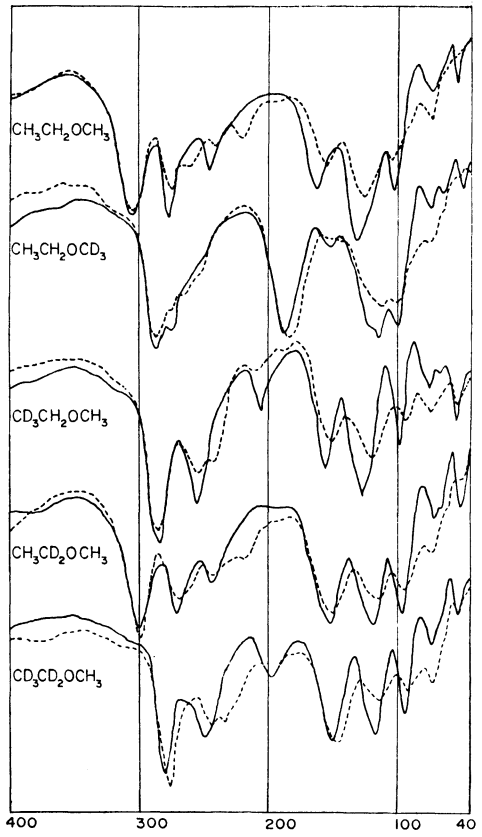

Fig. 2. Far infrared spectra of the solid phase (77°K) of ethyl methyl ether; broken line: deposited unannealed film, and solid line: annealed crystalline film.

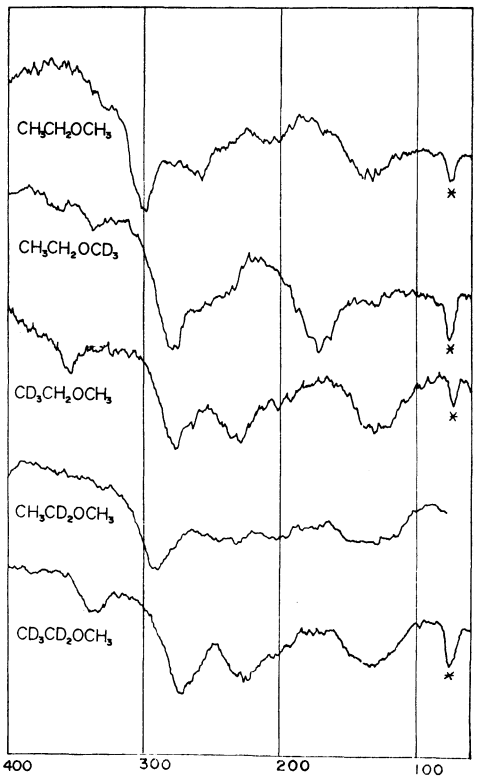

Fig. 3. Far infrared spectra of the liquid phase (~170°K) of ethyl methyl ether. The cell thickness is 0.2 mm. The band marked with * is due to polyethylene sheets.

Gas Spectra. Far infrared spectra of the gas phase (500 mmHg at room temperature) were measured with a 14 cm gas cell. Gas spectra (Fig. 4) are more complex than liquid and solid spectra, because of rotational structures and of overlapping hot bands.

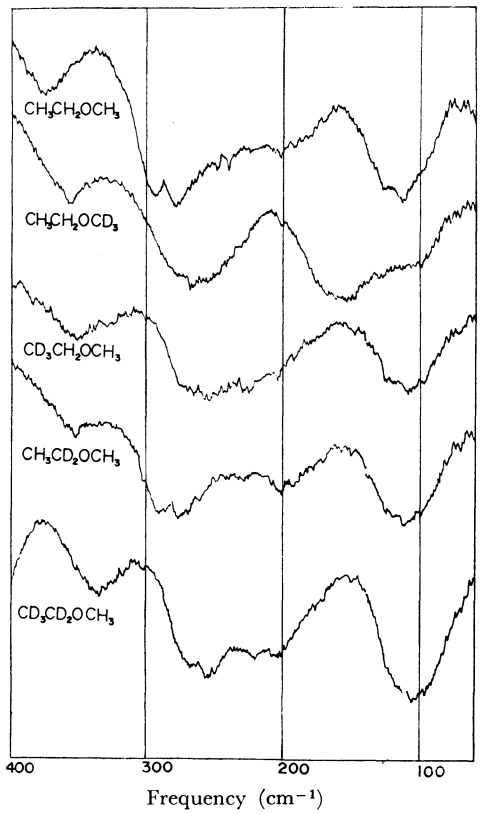

Fig. 4. Far infrared spectra of the gas phase (500 mmHg at room temperatrure) of ethyl methyl ether. The path length is 4 cm.

Solution Spectra. Infrared spectra (500~250 cm^{-1}) of ethyl methyl ether in carbon-tetrachloride solution were measured with a sealed KRS-5 cell (0.2 mm thick). Far infrared spectra of $CH_3CH_2OCH_3$ and $CH_3CH_2OCD_3$ in carbon-tetrachloride solution were measured with a sealed polyethylene cell (0.5 mm thick). Frequencies observed in solution are listed in Table 1, together with the frequencies observed for the solid, liquid, and gas phases.

Normal Vibration Treatments

The normal vibrations of the five isotopic species (d_0, d_3, d_3', d_2, and d_5) of ethyl methyl ether were treated with Wilson's ***GF*** matrix method[11]. In constructing inverse-kinetic energy matrices (***G***), the bond lengths of r(C-C)=1.530 Å, r(C-O)=1.420 Å, and r(C-H)=1.093 Å, tetrahedral bond angles, and the internal-rotation angles of 180°(trans) and 60°(gauche) were used. For the C-H stretching and deformation modes of the CH_3-C, C-CH_2-O, and O-CH_3 groups, local-symmetry coordinates (σ)[12] were used, together with the C-C and O-C stretching, C-O-C bending (ϕ), and internal-rotation coordinates (t).[13]

The potential energy matrices (***F***) were constructed on the basis of a generalized potential function, namely, the local-symmetry force field[12]. The initial set of potential constants of the CH_3-C, C-CH_2-O, and O-CH_3 groups were transferred from ethane[14], polyethylene glycol[15] and dimethyl ether[16], respectively, and were adjusted by the method of least squares[17] with reference to the infrared frequencies observed for the trans and gauche isomers of the five isotopic species (except for internal-rotation frequencies of the gauche isomer)[18]. After six cycles of adjustments, a converged set of potential constants was obtained. However, in the high frequency region (3000~600 cm^{-1}), a unique set of vibrational assignments of the five isotopic species were not yet established. On the other hand, in the low frequency region (<600 cm^{-1}), vibrational assignments were made satisfactorily, and a reliable set of potential constants was obtained for low-frequency modes; $f[\sigma(\text{C-C-O})]=0.925$, $f[\phi(\text{C-O-C})]=1.373$, $f[\sigma(\text{C-C-O})\cdot\phi(\text{C-O-C})]=0.167$, $f[t(\text{CH}_3\text{-CH}_2)]=0.0939$, $f[t(\text{CH}_2\text{-O})]=0.0769$, $f[t(\text{O-CH}_3)]=0.0682$ mdyn Å/rad², where three force constants were set as $f[r(\text{C-C})\cdot\sigma(\text{C-C-O})]=0.017$, $f[r(\text{C-O})\cdot\delta(\text{C-C-O})]=0.455$ and $f[r(\text{O-C})\cdot\phi(\text{C-O-C})]=0.259$ mdyn/rad.[15] Calculated frequencies lower than 600 cm^{-1} are listed in Table 1.

Lattice Vibrations

Far infrared spectra of the crystal, liquid and vapor phases of $CH_3CH_2OCH_3$ are shown in Fig. 5. In the lowest frequency region, the crystal bands at 52, 67, and 102 cm^{-1} disappear on melting and accordingly are assigned to lattice vibrations. On the other hand, the vapor band at 115 cm^{-1} corresponds to the liquid band at 132 cm^{-1} and to the crystal band at 166 cm^{-1}, since low-frequency internal-rotation vibrations are known to shift appreciably to higher frequency on phase-changes gas→liquid→crystal. Accordingly, the crystal band at 132 cm^{-1} is assigned to a lattice vibration, possibly coupled with internal-rotation modes. Observed frequencies of lattice vibrations of ethyl methyl ether (ν_0) and deuterated species (ν) and their ratios (ν_0/ν) are listed in Table 2.

In the crystal of ethyl methyl ether, the molecule does not have the center of symmetry, and, in principle, translatory and rotatory lattice modes are not separated from each other. However, for 'purely' translatory or rotatory vibrations, frequencies of isotopic molecules would be inversely proportional to the square root of the molecular mass or principal moments of inertia[8],

11) E. B. Wilson, *J. Chem. Phys.*, **7**, 1047 (1939); **9**, 76 (1941).
12) T. Shimanouchi, *Nippon Kagaku Zasshi*, **86**, 261 (1965); "Physical Chemistry", Vol. 4, ed., by H. Eyring, Academic Press, New York, N. Y. (1970), p. 233.
13) T. Miyazawa and K. Fukushima, *J. Mol. Spectry.*, **15**, 308 (1965).
14) J. I. Duncan, *Spectrochim. Acta*, **20**, 1197 (1964).
15) H. Matsuura and T. Miyazawa, This Bulletin, **41**, 1798 (1968).
16) H. Sugeta, Dissertation, Osaka University (1969).
17) D. E. Mann, T. Shimanouchi, J. H. Meal, and L. Fano, *J. Chem. Phys.*, **27**, 43 (1957).
18) K. Ohno, to be published separately.

TABLE 1. INFRARED FREQUENCIES[a] OF ETHYL METHYL ETHER IN THE CRYSTAL, LIQUID, AND GAS PHASES AND CARBON TETRACHLORIDE SOLUTION, CALCULATED FREQUENCIES, AND VIBRATIONAL ASSIGNMENTS

Species	Crystal	Liquid	Solution	Gas	Calc[b]	Assignment[c]
$CH_3CH_2OCH_3$	472 (m)		467 (s)	465 (s)	477 (T)	ϕ_s
					475 (G)	ϕ_a
	—	378 (vw)	376 (m)	374 (w)	375 (G)	ϕ_s
	310 (s)	300 (s)	299 (m)	287 (s)[d]	290 (T)	ϕ_a
	280 (s)	258 (m)	255 (vw)	248 (m)	252 (T)	$t(CH_3\text{-}CH_2)$
	—	240 (vw)	239 (w)	239 (m)	224 (G)	$t(CH_3\text{-}CH_2)$
	249 (m)	208 (w)	~200 (w)	202 (m)	201 (T)	$t(O\text{-}CH_3)$
				192 (w)	197 (G)	$t(O\text{-}CH_3)$
	166 (m)	132 (m)	~127 (w)	115 (s, b)	113 (T)	$t(CH_2\text{-}O)$
					112 (G)	$t(CH_2\text{-}O)$
$CH_3CH_2OCD_3$	449 (m)		448 (s)	451 (s)	452 (T)	ϕ_s
					452 (G)	ϕ_a
	—	360 (vw)	360 (m)	356 (w)	360 (G)	ϕ_s
	290 (s)	276 (s)	279 (m)	265 (s)[d]	273 (T)	ϕ^a
	277 (s)	258 (w)	246 (vw)	241 (w)	247 (T)	$t(CH_3\text{-}CH_2)$
	—	244 (w)		231 (w)	221 (G)	$t(CH_3\text{-}CH_2)$
	191 (s)	172 (m)	~165 (w)	155 (s, b)	156 (T)	$t(O\text{-}CD_3)$
					150 (G)	$t(O\text{-}CD_3)$
	155 (w)	129 (vw)	126 (w)	104 (m, b)	105 (T)	$t(CH_2\text{-}O)$
					100 (G)	$t(CH_2\text{-}O)$
$CD_3CH_2OCH_3$	446 (m)		439 (s)	436 (s)	455 (T)	ϕ_s
					460 (G)	ϕ_a
	—	353 (w)	356 (m)	350 (w)	355 (G)	ϕ_s
	285 (s)	276 (s)	278 (m)	262 (s)[d]	271 (T)	ϕ_a
	254 (m)	236 (m)		230 (m)	224 (T)	$t(O\text{-}CH_3)$
	—	228 (m)		225 (m)	195 (G)	$t(O\text{-}CH_3)$
	205 (w)	202 (w)		~175 (w, sh)	171 (T)	$t(CD_3\text{-}CH_2)$
	—	192 (vw)			167 (G)	$t(CD_3\text{-}CH_2)$
	155 (m)	129 (m, b)		108 (s, b)	109 (T)	$t(CH_2\text{-}O)$
					104 (G)	$t(CH_2\text{-}O)$
$CH_3CD_2OCH_3$	459 (m)		452 (s)	455 (s)	469 (T)	ϕ_s
					455 (G)	ϕ_a
	—	361 (vw)	358 (m)	351 (w)	353 (G)	ϕ_s
	303 (s)	292 (s)	294 (m)	282 (s)[d]	284 (T)	ϕ_a
	275 (m)	245 (w)		240 (vw)	245 (T)	$t(CH_3\text{-}CD_2)$
	—	233 (w)		229 (vw)	224 (G)	$t(CH_3\text{-}CD_2)$
	247 (m)	200 (w)		202 (w)	200 (T)	$t(O\text{-}CH_3)$
				193 (w)	197 (G)	$t(O\text{-}CH_3)$
	156 (s)	130 (m)		111 (b, s)	110 (T)	$t(CD_2\text{-}O)$
					108 (G)	$t(CD_2\text{-}O)$
$CD_3CD_2OCH_3$	437 (m)		419 (s)	416 (s)	448 (T)	ϕ_s
					436 (G)	ϕ_a
	—	336 (w)	342 (m)	336 (m)	338 (G)	ϕ_s
	282 (s)	272 (s)	268 (m)	260 (s)[d]	266 (T)	ϕ_a
	251 (m)	232 (m)		220 (m)	217 (T)	$t(O\text{-}CH_3)$
	—	226 (m)			195 (G)	$t(O\text{-}CH_3)$
	199 (w)	204 (w)		~170 (vw)	169 (T)	$t(CD_3\text{-}CD_2)$
	—	192 (w)			165 (G)	$t(CD_3\text{-}CD_2)$
	152 (m)	129 (m)		104 (s, b)	106 (T)	$t(CD_2\text{-}O)$
					102 (G)	$t(CD_2\text{-}O)$

a) Frequency in the cm^{-1} units; s: strong, m: medium, w: weak, vw: very weak, b: broad, sh: shoulder.
b) T: trans isomer, G: gauche isomer.
c) ϕ_s and ϕ_a are pseudo-symmetric and -antisymmetric skeletal bending modes, respectively, and t is internal-rotation mode.
d) Average frequency of the P and R branch-peaks.

Table 2. Observed frequencies[a] of lattice vibrations

Species	ν	ν_0/ν	ν	ν_0/ν	ν	ν_0/ν	ν	ν_0/ν
$CH_3CH_2OCH_3$	132	(1)	102	(1)	67	(1)	52	(1)
$CH_3CH_2OCD_3$	119 113	1.11 1.16	98	1.04	63	1.06	47	1.11
$CD_3CH_2OCH_3$	123	1.07	94	1.09	70	0.96	50	1.04
$CH_3CD_2OCH_3$	119	1.11	98	1.04	67	1.00	52	1.00
$CD_3CD_2OCH_3$	116	1.14	93	1.10	66	1.02	52	1.00

a) ν: in cm^{-1} unit, ν_0: frequency of $CH_3CH_2OCH_3$.

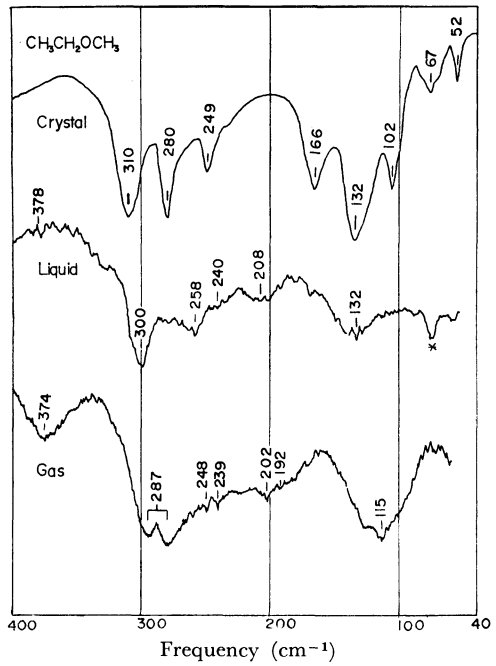

Fig. 5. Comparison of the far infrared spectra of the crystal, liquid, and vapor phases of ethyl methyl ether. The band marked with * is due to polyethylene sheets.

Table 3. Ratios of the square root of the molecular mass (M) and principal moments of inertia (I_a, I_b, and I_c) of the trans isomer[a]

Species	$(M/M^0)^{1/2}$	$(I_a/I_a^0)^{1/2}$	$(I_b/I_b^0)^{1/2}$	$(I_c/I_c^0)^{1/2}$
$CH_3CH_2OCH_3$	(1)	(1)	(1)	(1)
$CH_3CH_2OCD_3$	1.03	1.09	1.06	1.06
$CD_3CH_2OCH_3$	1.03	1.09	1.06	1.06
$CH_3CD_2OCH_3$	1.02	1.12	1.01	1.01
$CD_3CD_2OCH_3$	1.04	1.19	1.07	1.07

a) Ref. 8.

respectively. As shown in Table 3, frequency ratios of the translatory vibrations of ethyl methyl ether and deuterated species are as small as 1.02~1.04, whereas frequency ratios (1.01~1.19) of rotatory vibrations vary with deuterated species and rotation-axes. For the lattice vibration of $CH_3CH_2OCH_3$ (132 cm^{-1}), observed frequency ratios are as high as 1.07~1.14 (Table 2) and accordingly this highest-frequency lattice vibration is primarily due to a rotatory mode, possibly about the axis of the smallest moment of inertia (I_a).

Skeletal Deformation Vibrations

For the trans isomer of ethyl methyl ether CH_3-CH_2-O-CH_3, C-C-O and C-O-C bending vibrations are expected in the region below 600 cm^{-1}. In fact, infrared bands were observed at 472 and 310 cm^{-1} for the crystal phase. Since the mass of the oxygen atom is not much different from the mass of the methylene group, the C–C–O and C–O–C bending modes are hybridized, giving rise to the in-phase (ϕ_s) and out-of-phase (ϕ_a) bending modes. From normal vibration treatments, the bands at 472 and 310 cm^{-1} are assigned to ϕ_s and ϕ_a, respectively (Table 1). Skeletal bending vibrations of the trans isomer (point group C_s) belong to the A′ species and accordingly are expected to give rise to A, B, or AB hybrid bands in vapor spectra. In fact, the band of ethyl methyl ether at 287 cm^{-1} and corresponding bands of deuterated species are observed as B-type (Fig. 4).

The infrared band of liquid ethyl methyl ether at 378 cm^{-1} and corresponding bands of deuterated species disappear on crystallization, and accordingly are assigned to the gauche isomer (ϕ_s mode, Table 1). From normal vibration treatments[4,7], the other skeletal bending vibration (ϕ_a) of the gauche isomer of $CH_3CH_2OCH_3$ is expected at ~510 cm^{-1} but a corresponding band is not observed there. On the other hand, from the temperature dependence of the infrared intensities of the vapor bands at 465, 374, and 287 cm^{-1}, it was suggested[6] that the infrared band due to the ϕ_a vibration of the gauche isomer is overlapped by the band of the trans isomer at 465 cm^{-1}, although the intensity of the composite band is largely due to the gauche isomer. Corresponding bands are also observed for deuterated species (Table 1). It may be remarked that the potential term of $f[\sigma(\text{C-C-O})\cdot\phi(\text{C-O-C})]$ was necessary in least-square adjustments of potential constants with reference to skeletal-bending frequencies of the gauche isomer as well as of the trans isomer.

Internal Rotation Vibrations

For the trans isomer of ethyl methyl ether CH_3-CH_2-O-CH_3, the internal-rotation vibrations (CH_3-CH_2, CH_2-O, and O-CH_3) are all infrared-active. In fact, infrared bands are observed at 280, 249, and 166 cm^{-1} for the crystal phase (Fig. 6). The infrared band at 280 cm^{-1} is shifted appreciably to 205 cm^{-1} on deuteration of the CH_3-C group and is assigned to the internal-rotation vibration about the

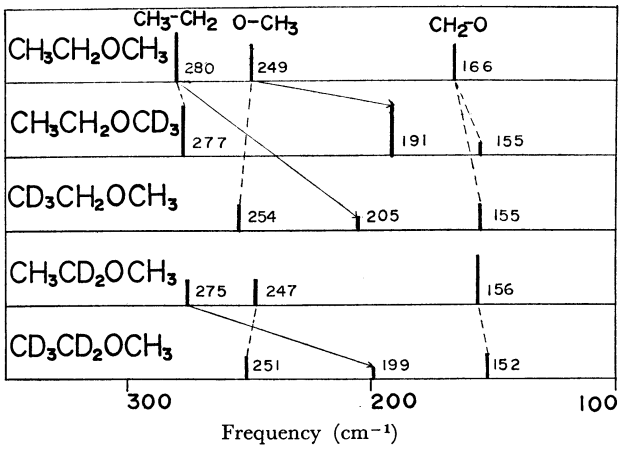

Fig. 6. Isotope shifts of internal-rotation frequencies of the crystal phase.

CH_3-CH_2 bond. On the other hand, the infrared band of $CH_3CH_2OCH_3$ at 249 cm^{-1} is shifted to 191 cm^{-1} on deuteration of the O-CH_3 group and is assigned to the internal-rotation vibration about the O-CH_3 bond. The low-frequency band at 166 cm^{-1} is shifted little on deuteration of the CH_3-C or O-CH_3 group and is assigned to the internal-rotation vibration about the CH_2-O bond. Similar deuteration effects are observed for the infrared bands of CH_3-CD_2OCH_3 at 275, 247, and 156 cm^{-1} (Fig. 6). Thus, the vibrational assignments of the intermal-rotation vibrations of the CH_3-CH_2 and O-CH_3 groups are established in the present study. Previous vibrational assignments[4,7] need be revised accordingly.

In the vapor phase, the internal-rotation vibrations of the trans isomer of $CH_3CH_2OCH_3$ give rise to sharp peaks (C-type) at 248, 202, and 115 cm^{-1}, just as expected for the transition moments parallel to the axis of the largest moment of inertia (I_c).

Internal-rotation frequencies of the gauche isomer are calculated to be lower than corresponding frequencies of the trans isomer (Table 1). Frequency differences between the trans and gauche isomers are due to the vibrational coupling between the internal-rotation modes and skeletal bending modes; such coupling is possible for the gauche isomer but not for the trans isomer.

Barrier Height for Internal Rotation of Methyl Group

For the trans isomer of ethyl methyl ether, three internal rotation modes belong to the same species (A″) and hybridization of those modes are expected. Accordingly, potential energy distributions[19] were calculated for internal-rotation vibrations as shown in Table 4. Hybridization of the internal-rotation modes of the CH_3-C and O-CH_3 groups is not negligible although these groups are separated by the central C-O bond. Accordingly, in estimating the barrier height of methyl groups, hybridization. of the two modes need be taken into account.

Table 4. Frequencies and potential energy distributions calculated for internal-rotation vibrations

Species	Freq. (cm^{-1})	Distribution (%)		
		CH_3-CH_2	CH_2-O	O-CH_3
$CH_3CH_2OCH_3$	252	70	0	20
	201	19	1	78
	113	0	95	1
$CH_3CH_2OCD_3$	247	91	0	7
	156	6	3	89
	105	0	93	4
$CD_3CH_2OCH_3$	224	25	1	74
	171	72	1	24
	109	0	95	1
$CH_3CD_2OCH_3$	245	82	0	17
	200	16	1	80
	110	0	96	2
$CD_3CD_2OCH_3$	217	20	1	78
	169	78	0	19
	106	0	95	2

In the present study, threefold potential barriers were estimated first with the harmonic approximation, $V_3(CH_3\text{-}C)=3.00$ and $V_3(O\text{-}CH_3)=2.18$ kcal/mol, from the force constants of $f[t(CH_3\text{-}CH_2)]=0.0939$ and $f[t(O\text{-}CH_3)]=0.0682$ mdyn Å/rad^2. Threefold potential barriers were also estimated as shown in Tables 5 and 6 (third column), with the single-top harmonic approximation, directly from infrared frequencies observed in the vapor phase (Table 1). The structural parameters[20] $F(CH_3\text{-}C)$ and $F(O\text{-}CH_3)$ were calculated (Tables 5 and 6, second column) from the same molecular parameters as used in normal vibration treatments [essentially the same F values were also obtained by the use of the molecular parameters determined by microwave analyses[8]]. Then, with reference to the V_3 values estimated from force constants, the corrections for the single-top approximation were calculated as shown in Tables 5 and 6 (fourth column).

In the second step, the anharmonicity of the three fold potential function was taken into account. Thus, Mathieu equation for the single-top case was used and the V_3 values were calculated (Tables 5 and 6, fifth column) from infrared frequencies of the vapor phase. Finally, the corrections for the single-top approximation were made, yielding corrected V_3 values as shown in the sixth column of Tables 5 and 6. It may be remarked that final V_3 values calculated for the five isotopic molecules agree closely with one another, giving mean values of

$$V_3(CH_3\text{-}C) = 3.3 \pm 0.1 \text{ kcal/mol}$$

$$V_3(O\text{-}CH_3) = 2.5 \pm 0.1 \text{ kcal/mol}$$

19) Y. Morino and K. Kuchitsu, *J. Chem. Phys.*, **20**, 1809 (1952); I. Nakagawa, *Nippon Kagaku Zasshi*, **74**, 243 (1953).

20) D. R. Herschbach, *J. Chem. Phys.*, **31**, 91 (1959).

Table 5. Structure parameters (F) and threefold potential barrier (V_3) of CH_3-C group

Species	F(cm^{-1})	V_3(kcal/mol)			
		Single-top harmonic	Corrected for single-top	Single-top Mathieu	Corrected barrier
$CH_3CH_2OCH_3$	6.18	3.16	−0.16	3.54	3.38
$CH_3CH_2OCD_3$	6.03	3.06	−0.06	3.42	3.36
$CD_3CH_2OCH_3$	3.54	2.75	+0.25	3.01	3.26
$CH_3CD_2OCH_3$	5.99	3.06	−0.06	3.42	3.36
$CD_3CD_2OCH_3$	3.35	2.74	+0.26	2.99	3.25

Table 6. Structure parameters (F) and threefold potential barrier (V_3) of O-CH_3 group

Species	F(cm^{-1})	V_3(kcal/mol)			
		Single-top harmonic	Corrected for single-top	Single-top Mathieu	Corrected barrier
$CH_3CH_2OCH_3$	6.18	2.10	+0.08	2.41	2.49
$CH_3CH_2OCD_3$	3.54	2.15	+0.03	2.38	2.41
$CD_3CH_2OCH_3$	6.03	2.79	−0.61	3.15	2.54
$CH_3CD_2OCH_3$	5.99	2.17	+0.01	2.49	2.50
$CD_3CD_2OCH_3$	5.89	2.61	−0.43	2.96	2.53

It is interesting to note that the threefold potential barrier of the CH_3-C group of ethyl methyl ether agrees closely with the corresponding barrier of propane[21], $V_3(CH_3\text{-}C)=3.325\pm0.020$ kcal/mol. Furthermore, the potential barrier of the O-CH_3 group of ethyl methyl ether agrees closely with the barrier of dimethyl ether recently determined from microwave analyses[22], $V_3(O\text{-}CH_3)=2.56$—2.60 kcal/mol.

21) E. Hirota, C. Matsumura, and Y. Morino, This Bulletin **40**, 1124 (1967).

22) M. Hayashi, private communication.